

Hot Strip Processing of Low Carbon Enameling Grades in the Range of 600 to 700 °C

A. Van Cauter, J. Dilewijns, F. Hörzenberger, R.A. Hubert, and B.C. De Cooman

(Submitted 28 October 1998; in revised form 26 October 1999)

The processing of continuously cast low carbon steel grades for enameling usually requires a high coiling temperature. Low-temperature coiling, however, is required to ensure deep drawability. A steel composition characterized by low AlN leads to a material combining both good formability and enameling ratio for hot strip coiling temperatures in the range of 600 to 700 °C. The influence of the coiling temperature on the mechanical properties, cementite morphology, H permeation, and enamel adhesion was studied in detail.

Keywords continuous casting coatings, coiling, enameling, steels

1. Introduction

Continuously cast steels are replacing the more traditional stabilized ingot cast grades in enameling applications. Ingot cast grades are characterized by a better compositional and structural homogeneity. They have a better internal purity with fewer inclusions. The inclusions present in stabilized ingot cast grades for enameling guarantee an efficient hydrogen (H) trapping, and consequently, their use results in the absence of fish scaling. The excellent enameling characteristics are also due to the high surface purity, which results in the absence of typical enameling defects, such as carbon boiling. This superior enameling can be combined with good press formability by using low coiling temperatures after the hot rolling.

The same combination of excellent deep drawability and enameling characteristic of the stabilized ingot cast grades for enameling cannot easily be achieved for continuously cast low carbon steels.

Low carbon enameling grades require a relatively high coiling temperature (CT) in order to have cementite (Fe_3C) coalescence. This coarse Fe_3C is broken during cold rolling, thereby creating voids acting as effective irreversible H trapping sites. At high coiling temperature, however, the aluminum nitride (AlN) also precipitates in the coiled strips. This AlN precipitation should take place during batch annealing in order to get a steel with improved deep drawability characteristics. This is due to the fact that the AlN precipitation stimulates the development of the favorable {111}-fiber texture,^[1] which results in a high normal anisotropy. However, it is possible to keep an appreciable amount of AlN in solution at the relatively high coiling temperatures, which will yield coarse carbides. This can be achieved for steels with a chemical composition with a lower AlN atomic ratio. The kinetics of the formation of AlN is mainly controlled by the diffusion of the Al atoms and the AlN ratio. This ratio has to be larger than one, to obtain an aging-free steel. Typical AlN ratios for low carbon

enameling grades are between 3 and 5. This corresponds typically to, e.g., an Al_{tot} content around 400 ppm and a N concentration of approximately 40 ppm. The present work concentrates on enameling steels with a lower AlN ratio. The particular range of the Al/N ratio for these steels is graphically represented in Fig. 1. The lower Al/N ratio is obtained by choosing a high N content and a low Al content to influence the AlN precipitation. A low Al amount retards the AlN-precipitation kinetics during coiling, because the Al diffusion coefficient is much smaller than the N diffusion coefficient. With a high N amount, some interstitial N is left in solution after coiling. In this way, it is possible to keep some Al and N in solution after coiling even at relatively high coiling temperatures. The free Al and N are available to form AlN precipitates during batch annealing so that a texture favorable for press formability is achieved. Figure 2 gives a simulation of the AlN precipitation during coiling. The model used for this theoretical calculation has been presented elsewhere by Hubert.^[2] For an Al content of 260 ppm and 65 ppm N, about 15 ppm N remains in solution for a coiling temperature of 650 °C, if a mean distance between the AlN precipitates of 0.24 μm is assumed. Figure 3 gives the interstitial nitrogen content after coiling as a function of the coiling temperature. Nuclei formation is not taken into account in this model. The precipitate density is based on transmission electron microscopy observations. The model calculations show

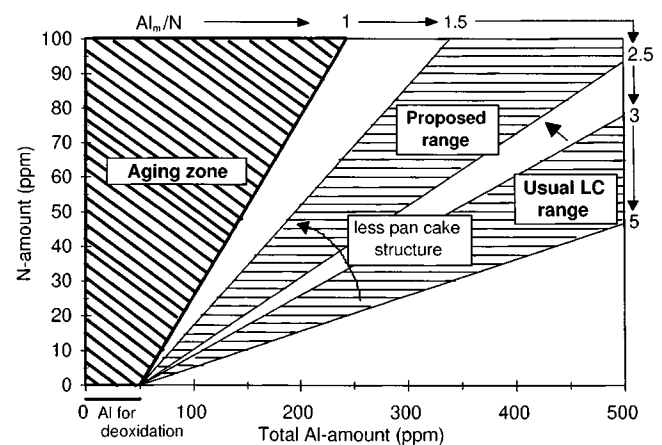


Fig. 1 Schematic of the proposed Al/N-ratio range for low carbon enameling steels combining formability and enameling

A. Van Cauter and J. Dilewijns, Laboratory for Iron and Steel-making, University of Ghent, B-9052 Zwijnaarde (Ghent), Belgium. F. Hörzenberger, R.A. Hubert, and B.C. De Cooman, Ocas N. V., Research Centre of the Sidmar Group, B-9060 Zelzate, Belgium.

for enameling. Steel C contains a higher Cu quantity, to see the influence of Cu on the enameling properties. In the literature, there is no uniformity about the influence of a higher Cu content in the steel on the pickling behavior. According to some authors,^[3-6] an increased Cu content causes a lower pickling rate, because Cu enriches at the steel surface during pickling and slows down the anodic reaction (the iron dissolution). Moreover, Cu interacts with S to form Cu₂S^[6] (and/or CuS). This compound precipitates on the steel surface and the sulfur is not available anymore for the formation of corrosion accelerating SH⁻ ions. Other authors^[7] mention an increased pickling rate for higher Cu content, because the pickling deposition is cathodic with respect to the steel, which causes an accelerated attack of the steel.

The processing parameters used for the laboratory processing are shown in Table 2. The coiling temperature was varied between 600 and 775 °C. After hot rolling, the sheets were either air cooled or water cooled to the coiling temperature.

The Ar₁ temperatures of the steels were measured using a THETA (Port Washington, NY) Dilatronic III S dilatometer equipped with a device allowing for deformation in compression. The compression specimens were solid cylinders with outer diameter of 3.5 mm and length of 5 mm. Temperatures were measured through a thermocouple spot welded to the specimens.

The distribution and structure of the cementite was studied by light optical microscopy and scanning electron microscopy (SEM) using a Zeiss (Oberkochen, Germany) DSM 962.

The amount of N in solution in the hot-rolled material was determined by the internal friction measurements, using a 40 kHz automatic piezoelectric ultrasonic composite oscillator technique.^[8-12] The mechanical properties were determined by means of tensile tests.

The resistance to fish scales was determined by measuring the hydrogen permeation time of the steel with a Ströhlein (Kaarst, Germany) apparatus. A thickness-independent hydrogen permeation value, t/d^2 , where t is the hydrogen permeation time in minutes and d the thickness of the steel in millimeters, was calculated. A high hydrogen index, t/d^2 , is usually taken as a measure of a better resistance against fish scales. In industrial practice, a hydrogen index higher than 6.7 min/mm² is required.

Panels of 8 × 40 cm were enameled by the two-coat/two-fire technique using an industrial enamel used in sanitary ware man-

ufacturing. The enamel was applied by wet spraying. The temperature dependence of the adherence was studied by means of strips placed in a gradient furnace, which allowed firing a single sample in the temperature range 780 to 860 °C.

The adherence of the enamel to the sheet was tested by a conventional impact test, according to the EN10209 standard. The impact mass of 1500 g was dropped from a height of 750 mm. The surface tested was compared with the standard table according to standard EN10209 and ratings from 1 to 5 were given (1: excellent adherence; and 5: total lack of adherence). Finally, the interface between steel and enamel was studied with a JEOL JXA 8800 L electron probe microanalyzer (EPMA), equipped with wavelength dispersive X-ray fluorescence analysis (supplied by Japan Electron Optics Ltd., Tokyo).

3. Results

The temperature dependence of the two main properties, cementite morphology and solute nitrogen concentration, was studied in detail. The difference in cementite morphology is shown in Fig. 4.

The study of the cementite structure with the optical microscope revealed that there was a significant difference between the cementite structure in the materials with CT higher than 700 °C and these with CT under 700 °C. At high CT, coarse cementite clusters are observed, whereas at low CT, the grain boundary cementite is much finer and more uniformly distributed. This difference was visible in both the hot-rolled material and the final cold-rolled sheet. The change in cementite morphology was not gradual but rather abrupt around 700 °C. The difference in cementite structure was caused by the value of the coiling temperature with respect to the Ar₁ temperature. If the CT is higher than the Ar₁ temperature, the transformation of austenite to ferrite has not finished before coiling. During coiling, the austenite, which has a higher C solubility than ferrite, enriches in carbon. After transformation, cementite clusters appear. On the other hand, when the CT is lower than the Ar₁ temperature, all austenite is transformed to ferrite before coiling starts. So there is no enrichment of carbon and all cementite is present as fine grain boundary cementite.

The interstitial N in the hot-rolled material was measured by internal friction for the materials with CT between 600 and 700 °C. There was no interstitial N for CT higher than 700 °C. At these high coiling temperatures, all N precipitated during coiling. However, there was still N in solution for coiling temperatures lower than 700 °C. Figure 5 gives the results for the three tested steels. The results of the model calculations of the interstitial N content are also shown for comparison. In the modeling, two mean interprecipitate distances were chosen, namely, $d = 0.2$ and $0.4 \mu\text{m}$. There was a good agreement between the measurements and the prediction of the simulation, except for CT lower than 600 °C. Here, the model predicted a higher amount of N in solution for the chosen distance between the AIN precipitates. This is very likely due to the estimated mean interprecipitate distance (0.2 or $0.4 \mu\text{m}$) in the model, which is too large for the situation with CT 600 °C. A low CT promotes the nucleation, so many nuclei are formed and the distance between the precipitates diminishes. As discussed in the Introduction, the modeling does not take the nuclei formation into account, which is why the mean interprecipitate distance has

Table 1 Nominal steel analysis range (ppm)

| Steel | C | Mn | P | N | Al _m | Cu |
|-------|---------|-----------|---------|-------|-----------------|---------|
| A, B | 480–500 | 2250–2500 | 100–150 | 50–80 | 200–300 | 175–200 |
| C | 480–500 | 2250–2500 | 100–150 | 50–80 | 200–300 | ≈400 |

Table 2 Processing of the material

| | |
|---------------------|---|
| Reheating furnace ↓ | SRT = 1250 °C |
| Hot rolling ↓ | 25 → 6 mm four rolling steps reduction 76% RFT > Ar ₃ |
| Coiling ↓ | 775 °C 675 °C 750 °C 650 °C 725 °C 625 °C 700 °C 600 °C |
| Cold rolling ↓ | 6 mm → 2, 7 mm reduction 55% |
| BA ↓ | batch annealing under argon atmosphere |
| Skin pass | 1% |

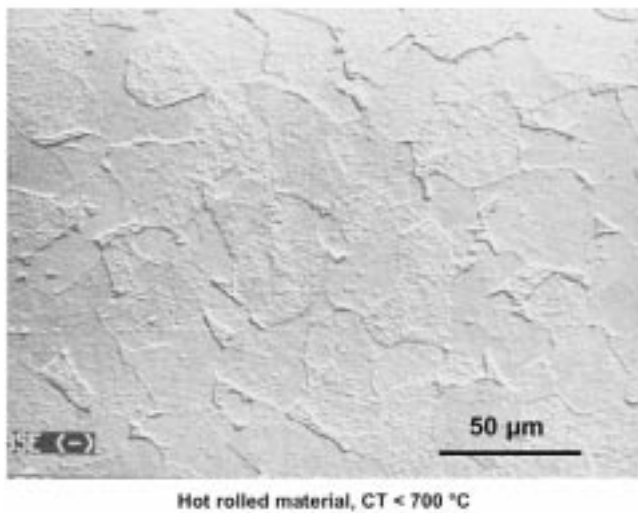
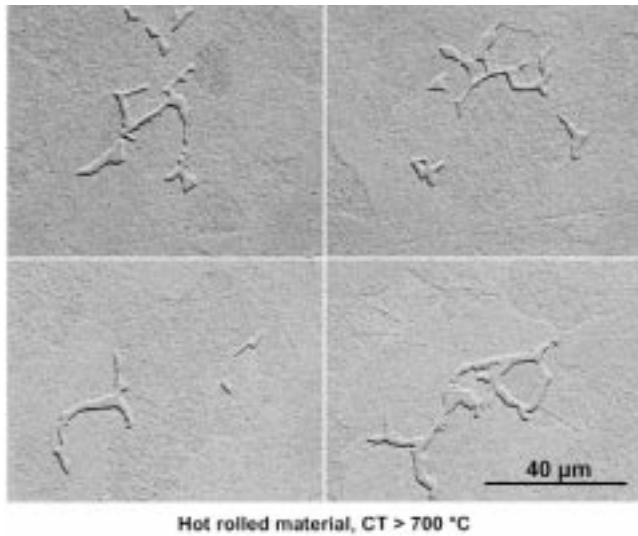


Fig. 4 Cementite morphology

to be estimated. Therefore, at low CT, a mean interprecipitate distance smaller than $0.2 \mu\text{m}$ should be chosen to obtain a good agreement between the model and the experimental results for the interstitial N content.

With a dilatometer, the A_{r1} temperature of steels A and C (higher Cu content) was determined at different cooling rates. Samples were heated to $1250 \text{ }^\circ\text{C}$ at a rate of $10 \text{ }^\circ\text{C/s}$. After a retention time of 2 min at $1250 \text{ }^\circ\text{C}$, the samples were cooled to $1130 \text{ }^\circ\text{C}$ at a rate of $10 \text{ }^\circ\text{C/s}$. At $1130 \text{ }^\circ\text{C}$, a 10% deformation was given. The samples were then further cooled at rates varying from 2 to $30 \text{ }^\circ\text{C/s}$. A constant cooling rate was applied, whereby the furnace temperature control compensated for the heating due to the $\gamma \rightarrow \alpha$ transformation. Figure 6 gives the results.

A cooling rate of $2 \text{ }^\circ\text{C/s}$ is typically obtained with air cooling. According to Fig. 6, the A_{r1} temperature is $707 \text{ }^\circ\text{C}$ in this case. This is in agreement with the observations of a change in the cementite morphology around $700 \text{ }^\circ\text{C}$. At higher cooling rates, the A_{r1} temperature is lower. For the same cooling rate, an increase

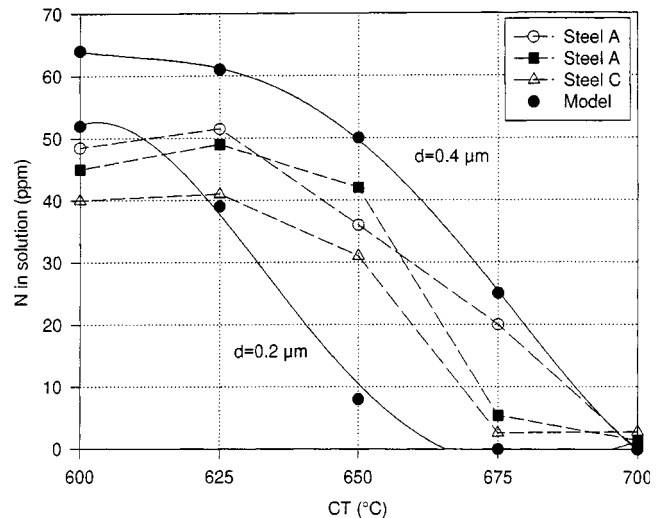


Fig. 5 Results of the interstitial N measurements on the hot-rolled strip

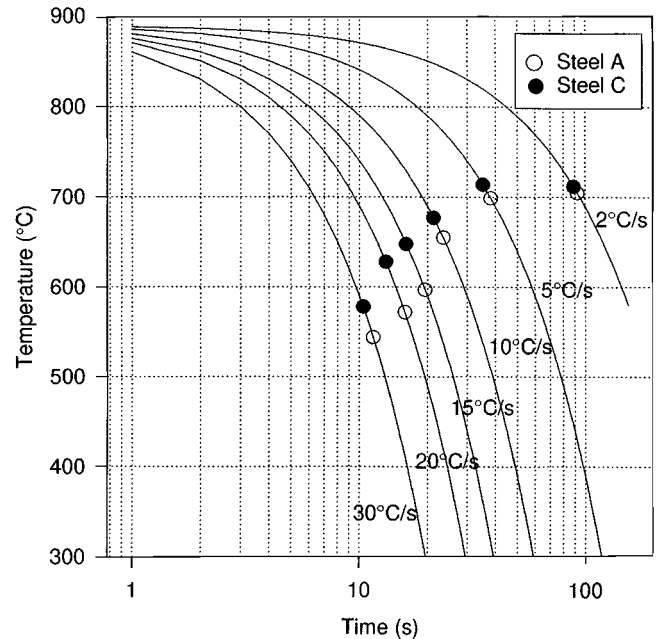


Fig. 6 Influence of the cooling rate on the A_{r1} temperature

in Cu content in the steel (C) results in a higher A_{r1} temperature. The fact that the CT has to be higher than the A_{r1} temperature for good enameling characteristics, but that good mechanical properties require a low CT, means that steels with a low Cu content should be favored.

There was no distinction in grain size for the different coiling temperatures in the hot-rolled sheet; the grain size was ASTM grain size 8 in all cases. There were no pancake grains visible on the cold-rolled samples with CT higher than $700 \text{ }^\circ\text{C}$. There was a clear pancake structure for the materials with lower CT. Figure 7 shows the microstructure of the material coiled at CT lower than $700 \text{ }^\circ\text{C}$ and of the material with CT higher than $700 \text{ }^\circ\text{C}$. Table 3 summarizes the mechanical properties.

A higher CT causes a decrease of R_e and R_m and an increase of A_{80} . The CT has also a positive influence on the n value. The r value decreases when the CT rises as expected, since high coiling temperatures are detrimental for deep drawability.

The hydrogen permeation time of each material was measured with the Ströhlein equipment. Figure 8 gives the results of the permeation index, t/d^2 , as a function of the coiling temperature.

Table 3 Influence of the coiling temperature on R_e , R_m , A_{80} , n_{90° , and the r values ($d = 2.7$ mm, batch annealed material)

| CT (°C) | R_e (MPa) | R_m (MPa) | A_{80} (%) | n_{90° | r_{90° | r_{0° | r_{45° | r_{mm} |
|---------|-------------|-------------|--------------|----------------|----------------|---------------|----------------|----------|
| 775 | 178 | 306 | 44.1 | 0.226 | 1.53 | 1.31 | 0.84 | 1.13 |
| 750 | 177 | 306 | 44.1 | 0.226 | 1.47 | 1.28 | 0.85 | 1.11 |
| 725 | 180 | 310 | 42.1 | 0.226 | 1.47 | 1.33 | 0.85 | 1.01 |
| 700 | 194 | 315 | 41.6 | 0.221 | 1.58 | 1.23 | 0.83 | 1.09 |
| 675 | 165 | 310 | 41.8 | 0.217 | 1.51 | 1.36 | 1.03 | 1.23 |
| 650 | 185 | 317 | 40.0 | 0.205 | 1.66 | 1.62 | 1.02 | 1.33 |
| 625 | 190 | 319 | 38.4 | 0.202 | 1.82 | 1.65 | 1.06 | 1.40 |
| 600 | 204 | 319 | 38.2 | 0.201 | 1.76 | 1.63 | 1.02 | 1.37 |

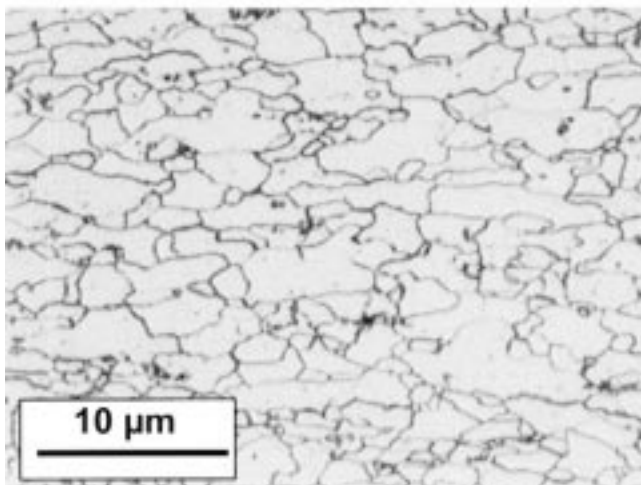
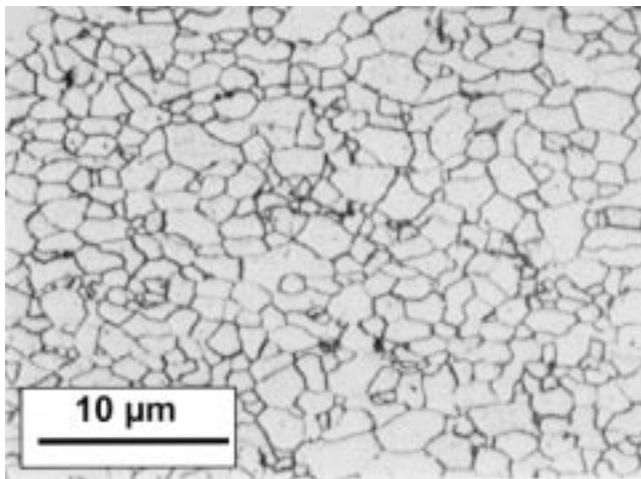


Fig. 7 Microstructure of the cold-rolled and annealed material: top: CT > 700 °C; and bottom: CT < 700 °C

For the material that was air cooled after hot rolling, there is a sharp improvement of the hydrogen index around a CT of 700 °C. This coincides precisely with the change from grain boundary cementite (CT < 700 °C) to coarse cementite clusters (CT > 700 °C). It has to be noted that the coiling temperature at which the cementite morphology changes is lower when the material is water cooled with a higher cooling rate after hot rolling instead of air cooled. So, the water-cooled material still has a higher hydrogen index at low coiling temperatures.

Strips of the materials with CT between 600 and 700 °C were enameled. For each strip, five firing temperatures between 780 and 860 °C were used. Figure 9 gives the results of the impact test, and Fig. 10 shows the enameled panels after performing the impact test.

It can be seen that the adhesion improves at higher firing temperatures and higher coiling temperature. No special measures were taken to improve the adherence. When the plates are pickled before enameling, the adherence is considerably better. Comparing the results of the adherence tests for steels A and B with

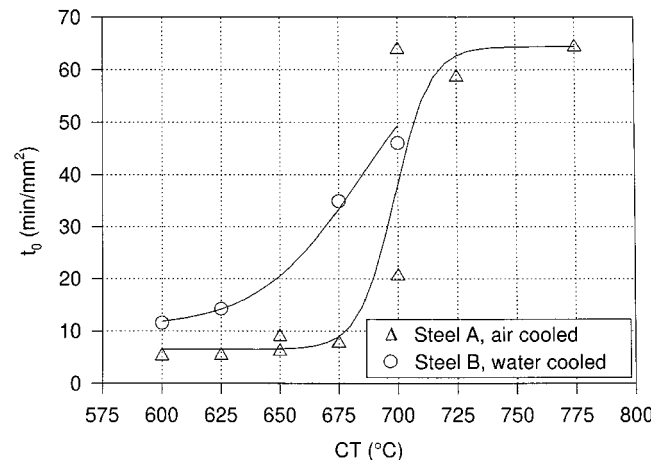


Fig. 8 Influence of the coiling temperature on the hydrogen permeation index t_0

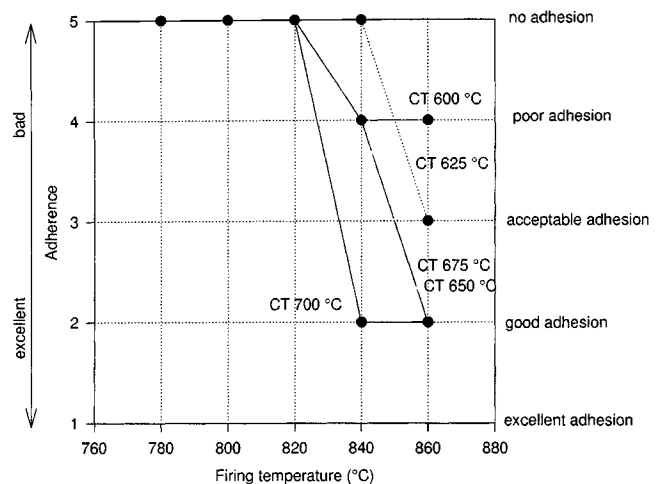


Fig. 9 Results of the impact test

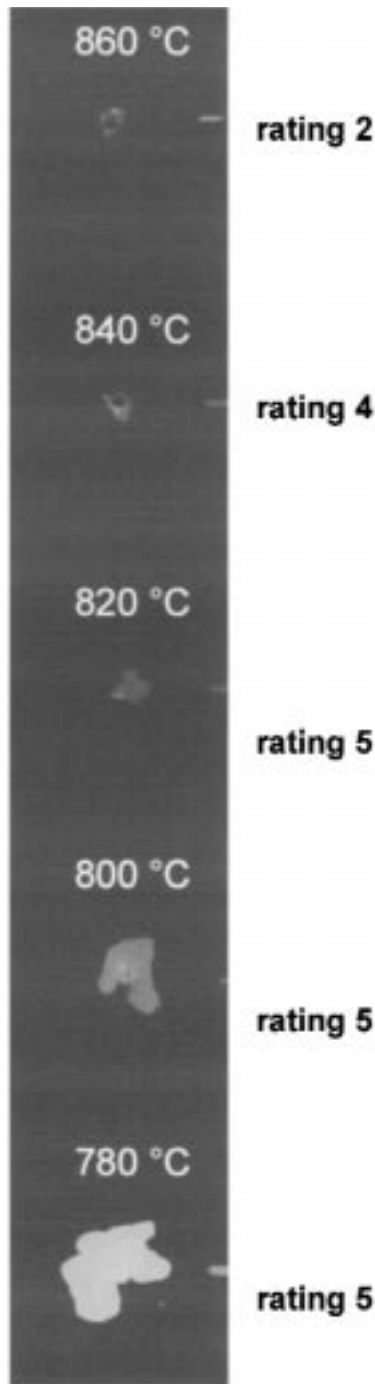


Fig. 10 Enameled samples after performing the impact test (CT - 650 °C)

steel C demonstrated that increasing the Cu content to 400 ppm did not influence the enamel adherence.

The enamel/steel interface was examined on cross sections by SEM. The results showed a well-developed steel/enamel interfacial adhesion layer for all steel substrates. This layer was a Fe-Co-Ni intermetallic layer characterized by a high roughness. Metallic Ni particles were detected throughout the enamel. This observation suggests that a substantial amount of the Ni²⁺ ions were reduced in the enamel. Due to the fact that these Ni parti-

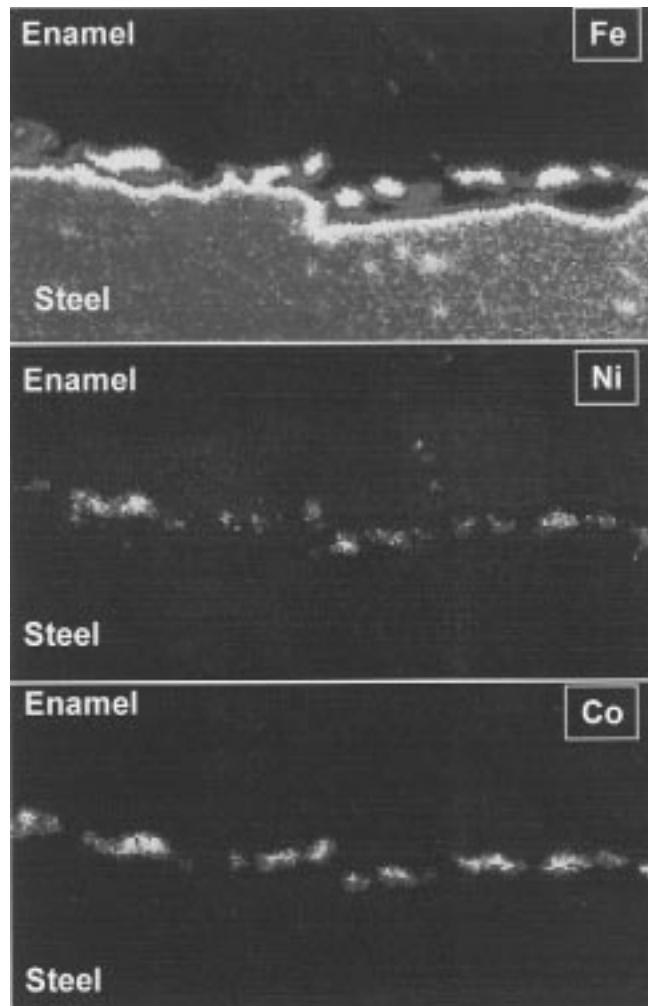


Fig. 11 EPMA scan of the steel/enamel interface

cles did not form at the enamel/steel interface, it is believed that Ni makes only a minor contribution to the adherence. The Co²⁺ ions were effectively reduced at the interface and formed an intermetallic FeCo interfacial adhesion layer containing small amounts of Ni. This can be clearly observed in the elemental mappings shown in Fig. 11.

4. Conclusions

The study of low carbon enameling grades with N and Al levels, adapted to optimize enameling and drawability has led to the following results.

- It is possible to combine good deep drawing characteristics and good enameling properties for continuously cast low carbon steels if the Al/N ratio is lower by applying a low Al and a high N concentration.
- The CT has to be higher than the Ar₁ temperature to obtain good enamelability. For air cooling, this temperature is 700 °C for this steel. However, the Ar₁ temperature can be reduced by

applying faster cooling after hot rolling. The A_{r1} temperature decreases at higher cooling rates, because both the nucleation rate and the growth are finite.^[9]

- At coiling temperatures higher than the A_{r1} temperature, coarse cementite clusters are found, which can be attributed to the presence of austenite when coiling starts. When the CT is higher than the A_{r1} temperature, all the austenite is transformed to ferrite before the coiling begins, and only free grain boundary cementite is formed. This difference in cementite structure is clearly visible in both hot-rolled and cold-rolled materials
- A higher CT has a positive effect on R_e , R_m , A_{80} , and n , but the r value decreases.
- The N can be kept in solution in the hot-rolled material at coiling temperatures lower than 700 °C.
- The enamel adhesion is improved by raising the CT and by increasing the firing temperature.
- Raising the Cu content to 400 ppm does not influence the enamel adherence.
- The A_{r1} temperature of the material can be lowered by applying a faster cooling on the runout table of the mill.
- A higher Cu content raises the A_{r1} temperature, which is undesirable because the CT has to be higher than the A_{r1} temperature to give good enameling characteristics. However, a low CT provides better mechanical properties and requires a low A_{r1} temperature. This means that a low Cu content is advantageous.

Acknowledgments

The authors thank Ir. I. Bultinck for the internal friction measurements and Dr. H. Storms for the EPMA analysis. The expert technical support of D. De Bruyn is also gratefully acknowledged.

References

1. W.B. Hutchinson: *Int. Met. Rev.*, 1984, vol. 29 (1), pp. 25-42.
2. R. Hubert: *ATB Metall.*, 1995, vol. 34-35, pp. 5-10.
3. J. Albrecht, H.-E. Bühler, and S. Baumgartl: *Arch. Eisenhüttenwes.*, 1974, Aug., pp. 561-65.
4. E. Riecke, B. Johnen, R. Möller, and H. J. Grabke: *Weerkstoffe Korr.*, 1985, vol. 36, pp. 435-54.
5. A. Dietzel, H. Warnke, and H. Dittmer: *Mitt. Vereins Deutscher Emailfachleute*, 1985, Dec., pp. 153-64.
6. F.M. Koch and K.-D. Rogausch: *Mitt. Vereins Deutscher Emailfachleute*, 1991, May, pp. 49-62.
7. A. Dietzel and H. Dittmer: *Arch. Eisenhüttenwes.*, 1984, Oct., pp. 483-86.
8. Z.-L. Pan, I.G. Ritchie, and H.K. Schmidt: Automatic Piezoelectric Ultrasonic Composite Oscillator Technique (APUCOT), User Manual, AECL Research, Whiteshell Laboratories, Pinawa, Manitoba, Canada.
9. I.G. Ritchie, Z.-L. Pan, K.W. Sprungmann, H.K. Schmidt, and R. Dutton: *Can. Met. Q.*, 1987, vol. 26, pp. 239-50.
10. K. Eloot and J. Dilewijns: *ISIJ Int.*, 1997, vol. 37 (6), pp. 604-14.
11. K. Eloot, L. Kestens, and Dilewijns: *ISIJ Int.*, 1997, vol. 37 (6), pp. 614-22.
12. K. Eloot, J. Dilewijns, C. Standaert, and B.C. De Cooman: *J. Magn. Magn. Mater.*, 1994, vol. 133, pp. 223-25.
13. L. Guillot, R. Tarrant, D. Rault, and M. Entringer: *Surfaces*, 1986, vol. 182, p. 27.
14. L. Guillot and Seurin: *PEI Meeting Atlanta*, July 1989, Vitreous Enameller, United Kingdom, 1989, p. 110.
15. W. Birmes, L. Meyer, and W. Warnecke: *Mitt. Vereins Deutscher Emailfachleute* 1974, vol. 22, H. 5, pp. 41-48.
16. W.C. Leslie, R.L. Rickett, C.I. Dotson, and C.S. Walton: *Trans. ASM*, 1954, vol. 46, pp. 1470-99.
17. G. Papp, G. Giedenbacher, K. Kösters, and F. Wallner: *Mitt. Vereins Deutscher Emailfachleute* 1985, vol. 33, H. 3, pp. 25-36.
18. G. Papp, G. Giedenbacher, and F. Wallner: *Mitt. Vereins Deutscher Emailfachleute* 1987, vol. 35, H. 1.
19. F. Listhuber and E. Gieger: *Mitt. Vereins Deutscher Emailfachleute*, 1974, vol. 22, H. 2, pp. 13-24.
20. K. Ecker, G. Papp, G. Ernsthöfer, and G. Giedenbacher: *Mitt. Vereins Deutscher Emailfachleute* 1981, vol. 29, H. 11, pp. 143-56.